LBL-11816
Preprint

Lawrence Berkeley Laboratory
UNIVERSITY OF CALIFORNIA

Materials & Molecular
Research Division

Submitted to Nuclear Technology

BEHAVIOR OF METALLIC INCLUSIONS IN URANIUM DIOXIDE

Rosa L. Yang and D.R. Olander

March 1981

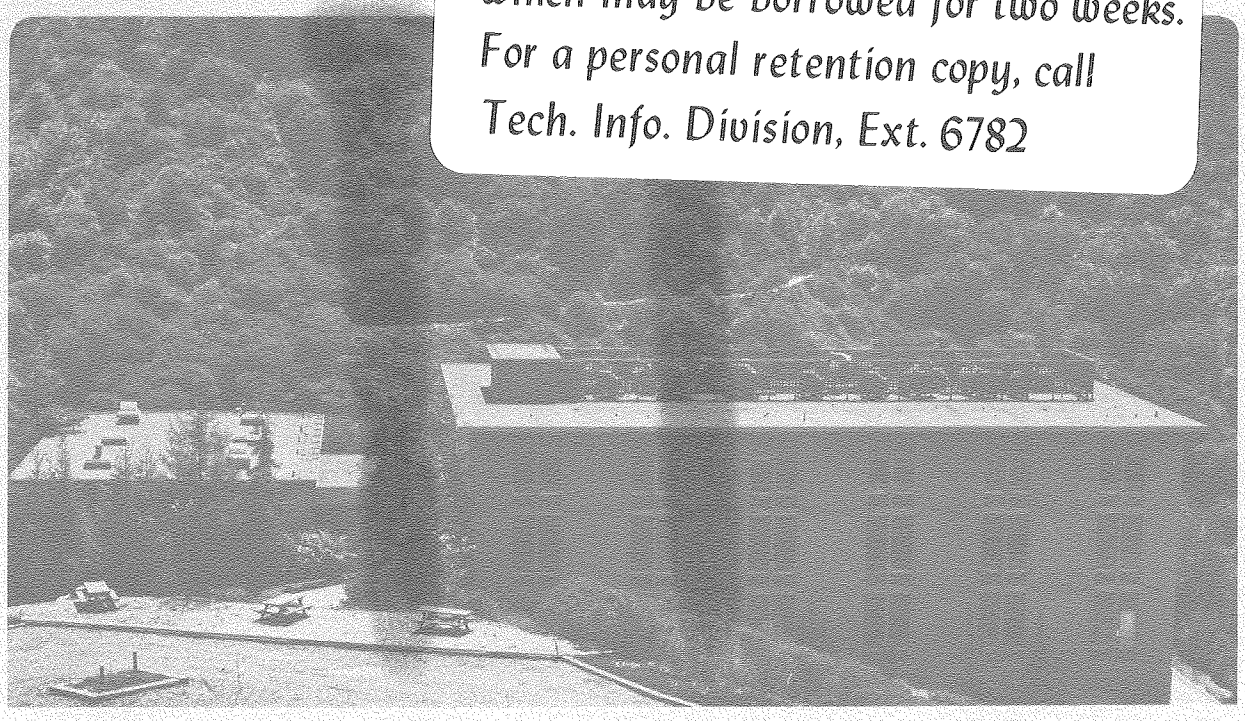

Prepared for the U.S. Department of Energy under Contract W-7405-ENG-48

DISCLAIMER

LBL-11816

BEHAVIOR OF METALLIC INCLUSIONS IN URANIUM DIOXIDE

by Rosa L. Yang and D.R. Olander

Materials and Molecular Research Division of the Lawrence Berkeley Laboratory and the Department of Nuclear Engineering of the University of California, Berkeley, CA 94720

ABSTRACT

The mobility of micron-size powders of refractory and noble metals in UO_2 was investigated under isothermal and temperature gradient conditions. The metal particles were initially placed between two polished surfaces of UO_2 and any movement which occurred during high temperature annealing was determined microscopically. Tungsten and molybdenum particles 1 to 10 μm in diameter were immobile in UO_2 at 2500°C in a temperature gradient of 1400°C/cm. Ruthenium, however, dissolved into and spread through hypostoichiometric, polycrystalline urania and was found after isothermal annealing as the U-Ru intermetallic compound in the grain boundaries of the oxide. The mechanism does not involve bodily motion of the metal particles. Rather, ruthenium dissolves in the grain boundaries of the oxide, migrates as atoms via the same pathway, and reacts while migrating to form URu_3. This product grows as layers in the grain boundaries. Isothermal ruthenium spreading followed simple diffusion theory, and apparent solubilities and effective diffusivities were obtained from the data for the temperature range 2000 to 2300°C. In a temperature gradient, ruthenium moves to the hot zones of UO_2; the mechanism appears to be the same as found for isothermal spreading, but the extent of movement up the temperature gradient cannot be explained by simple diffusion theory, even with an appreciable Soret effect.

I INTRODUCTION

Oxide nuclear fuels irradiated to high burnup develop precipitates of metallic fission products (1-7). These inclusions consist principally of molybdenum and ruthenium, with smaller quantities of technetium, palladium and rhodium. Occasionally uranium has been identified in these inclusions. The uranium is probably present as the intermetallic compound UM_3 (M = Ru, Rh, or Pd), which is the thermodynamically preferred state of the noble metals in UO_2 or $(U,Pu)O_2$ of sufficiently low oxygen potential. The inclusions take the form of particles with diameters less than $\sim$ 10 μm and are found in the equiaxed and columnar grain regions of the fuel. Occasionally large ingots of the metallic fission products are found attached to the wall of the central void of LMFBR fuels. It is widely believed that the inclusions move up the temperature gradient in much the same way as fission gas bubbles, that is by a surface diffusion mechanism (8). D'Annucci et al. (9) prepared uniform distributions of Ru and Mo inclusions in UO_2 and examined their behavior in a radial temperature gradient created by resistive heating of the specimen. They found that the small particles had sufficient mobility to coalesce into larger ones, but there was no evidence of biased migration up the temperature gradient. Michels and Poeppel (10) etched sections of irradiated mixed oxide fuel and observed trails behind metallic fission product inclusions; these trails were taken to represent the paths of the metal particles in the temperature gradient, and their lengths provided estimates of the inclusion velocities.

In order to obtain a clearer picture of the mobility of solid metallic inclusions in UO_2, we have studied the behavior of micron-sized metal particles initially located on an interior plane in a UO_2 pellet under both isothermal

conditions and in an axial temperature gradient. In addition to the geometry of the initial dispersion of metal particles in the ceramic, our experiments differ from those of D'Annucci et. al. (9) in the oxygen environment. Oxygen potentials sufficiently low to reduce urania were achieved. In this respect the present tests simulate conditions in the central zone of a mixed oxide fuel pin rendered oxygen-deficient by thermal redistribution.

II EXPERIMENTAL

A. Specimen Preparation

Sintered uranium dioxide pellets were obtained from the General Electric Company (Vallecitos Laboratory) with a density 98% of the theoretical value and an average grain size of 15 μm. The pellets were 1.2 cm in diameter and approximately the same height. A wafer ∿ 1 mm thick was sliced from a pellet and all end faces of the pellet and wafer were polished with a series of abrasives terminating with 6 μm diamond paste. Care was taken to maintain the faces parallel. The pellet and the wafer were later rejoined with a layer of metal powder in between.

The metals used to simulate the fission product inclusions were tungsten, molybdenum and ruthenium. Tungsten was chosen even though it is not a fission product because it was available as spherical particles in the 3 - 6 μm diameter range. The molybdenum and ruthenium powders were irregularly-shaped and tended to clump together when deposited on the UO_2 surface. Figure 1 shows typical deposits on the polished pellet face. A UO_2 wafer was placed on top of the metal deposit to complete the specimen assembly.

B. Isothermal Sintering

The pellet-wafer assembly with the metal particle layer was loaded into the sintering yoke shown in Fig. 2. This unit functioned as a type of hot-pressing apparatus, and had the following objectives: 1. To reduce the oxide to a stoichiometric or slightly hypostoichiometric state by heating in hydrogen. The metal particles tended to oxidize and disperse if specimens

were directly heated in a vacuum without the reduction step. 2. To seal the metal particles firmly in the UO_2 matrix and to eliminate the gap between the pellet and the interface. Incomplete closure of this interface might have impeded motion of the metal particles in subsequent thermal gradient testing. 3. To remove some of the porosity in the oxide. In a thermal gradient, the porosity migrated to the hot face of the apparatus where it produced a gap and a corresponding heat transfer resistance which prevented attainment of high temperatures.

The assembly was loaded compressively while at room temperature by tightening the tantalum nut in the molybdenum yoke shown in Fig. 2. The yoke was then suspended inside a resistance furnace where it was kept in hydrogen for 10 - 36 hours at temperatures between 2000 and 2300°C. At elevated temperatures, differential thermal expansion of the oxide and the refractory metal yoke increased the compressive stress. Figure 3 shows a section of the pellet-wafer interface following the treatment outlined above. The tungsten particles are seen to be well-embedded in the UO_2 and the gap has been eliminated.

C. Temperature Gradient Furnace

The pellet-wafer assembly, sintered with tungsten or molybdenum powder as described above, was loaded into the tungsten crucible shown in Fig. 4. When testing ruthenium particles in a temperature gradient, the isothermal sintering step was omitted for reasons explained later. The crucible shown in Fig. 4 consisted of a tube and top lid fabricated of tungsten by chemical vapor deposition. The lid had a spark-cut hole for temperature measurement. The pellet-wafer assembly fitted into the tube with a 30 μm radial clearance. After inserting the specimen and rhenium foil separator, the tantalum collar was electron-beam welded to the bottom of the tube.

The crucible containing the specimen was inserted into a thermal gradient furnace in which the top lid of the crucible was heated by electron bombardment in a vacuum and the bottom of the UO_2 pellet was cooled by a refractory metal rod. A thermocouple pressed against the pellet bottom and an optical pyrometer sighted on the hole in the top lid provided information from which the temperature distribution in the specimen was calculated by the HEATING-5 code.

A tight radial fit of the UO_2 specimens in the crucible was automatically assured by differential thermal expansion, which eliminated the small original radial gap. Even though the UO_2 specimen was pressed into the crucible by a yoke-type arrangement similar to that shown in Fig. 2 for the isothermal tests, performance of early versions of the apparatus was marred by the formation of void space between the upper UO_2 surface and the tungsten lid. This gap was shaped like a spherical indentation in the top of the UO_2 and was nearly 1 mm deep on the axis. However, contact between UO_2 and tungsten was good at the corner where the lid joined the tube. The volume of the gap corresponded roughly to the residual porosity of the UO_2 (including incomplete closure of the pellet-wafer interface) which experienced temperatures above $\sim$2000°C during the experiment. Because of radiation from the sides, the tungsten lid close to the axis was hotter than the peripheral zones. Consequently the porosity moved towards the axis in addition to moving upwards and so the void formed in the shape of a spherical segment. Numerical analysis of the temperature distribution in the crucible, with radiant heat transfer across the gap, indicated a > 200°C temperature drop between the bottom of the tungsten lid and the top UO_2 surface. This thermal limitation, plus the fact that the gap was so deep that the metal powder layer near

the axis was exposed by formation of the void, was remedied by the following measures: 1. using a tungsten crucible with a wall thickness of 1.14 mm instead of the original value of 0.4 mm; 2. winding the electron beam filament so that the periphery rather than the center of the tungsten lid was heated; 3. placing radiation shields around the top of the tungsten lid. These measures tended to reduce radial temperature gradients in the UO_2, so that the gap was created more uniformly over the top UO_2 surface. This redistribution of the voidage formed by pore migration reduced the depth of the gap on the axis to 1/10 of what it had been previously. The gap, however, could not be entirely eliminated.

Additional details of the experimental procedure can be found in Ref. 11.

III THERMAL GRADIENT ANNEALING OF UO_2 CONTAINING TUNGSTEN AND MOLYBDENUM

Several UO_2 pellet-wafer assemblies containing tungsten or molybdenum powder were prepared and tested as described in the previous section. During the thermal gradient annealing, the temperature measured in the hole in the tungsten lid was varied from 2400 to 2800°C while the temperature of the cold part of the UO_2 was between 1100 and 1200°C. The temperature gradients in the tests were between 1000 and 1400°C/cm and the temperature at the plane of the metallic inclusions was between 2100 and 2500°C. The duration of the tests varied from 8 to 36 hours. Following the thermal gradient anneal, each sample was cut longitudinally and the cross section examined by microscope to determine the extent of migration of the metal particles.

The position of the original layer was easily recognized on the photomicrographs because $\sim$ 95% of the particles experienced no detectable movement; there was no evidence of systematic biased displacement of the particles from the original plane. The few particles which were not on the original plane

were found a few tens of microns away from it, mostly in the direction of the hot part but occasionally towards the cool part of the sample. Figure 5 gives a typical view of the region near the original interface after thermal gradient treatment. The metal particles (white spots) which are not on the line representing the original plane were probably displaced because of asperities in the as-polished surfaces or because of local plastic deformation of the specimen while at high temperature. According to the surface diffusion mechanism of displacement in a thermal gradient (8), a particle 5 μm in diameter in a temperature gradient of 1300°C/cm at 2500°C should have moved 800 μm in 12 hours. This calculation includes a heat transfer resistance between the metal sphere and the ceramic as suggested by Michels and Poeppel (10). Our negative results clearly indicate that direct application of the theory developed for small bubbles in UO_2 does not apply to refractory metal particles in the same medium. Clearly it is inappropriate to use the surface diffusion coefficient of UO_2 to represent mobility of UO_2 molecules in the interface with a metal. The absence of movement of micron-size solid metal inclusions in a temperature gradient is consistent with the findings of D'Annucci et al. (9), but does not agree with Michels and Poeppel's interpretation of their observation of inclusion motion in irradiated fuel (10). Because theirs was an in-pile experiment, neither the thermal history of the fuel nor the composition of the metal phase could be controlled as closely as in a laboratory experiment. Uncertainties in both the fuel temperature during migration and in the melting point of the inclusions raise the possibility that the inclusions were liquid and not solid. If this were the case, mobility could have been due to transport of uranium through the inclusion rather than in the interface as required by the surface diffusion mechanism.

IV ISOTHERMAL ANNEALING OF UO_2 CONTAINING RUTHENIUM

Uranium dioxide specimens containing a plane of ruthenium powder were

isothermally sintered by the procedure described in Section IIB. The sintering temperature never exceeded the melting point of ruthenium (2310°C). After annealing, the specimen was removed from the sintering yoke and the surface parallel to the original plane of metal powder was polished and examined by optical microscope, x-ray fluorescence, and electron microprobe. This procedure was repeated a number of times, each polishing operation removing 50 - 100 microns, until the region within 1000 μm on both sides of the original plane of metal powder had been examined. As seen in Fig. 6, a white metallic phase nearly encapsulating the UO_2 grains was found at distances quite far from the original interface. Electron microprobe analysis showed that this phase contained uranium and ruthenium, but their ratio could not be determined accurately because of insufficient spatial resolution of the microprobe. No ruthenium was detected within the UO_2 grains.

An additional experiment was conducted to determine whether the ruthenium inclusions migrated as entities or whether the mechanism was one of solution of ruthenium in UO_2 followed by diffusion in atomic form. To clarify this point the ruthenium powders were replaced by a ruthenium disk ($\sim$ 0.076 cm thick). After a high temperature anneal, essentially the same type of ruthenium migration pattern as shown in Fig. 6 was observed. Since the ruthenium disk could not break up into small particles, ruthenium must dissolve into UO_2 and migrate as atoms.

In order to determine whether the diffusion process occurred via grain boundaries or in the UO_2 crystal lattice, ruthenium powder was placed between two UO_2 single crystal wafers and the assembly was annealed isothermally at 2250°C for 12 hours. Post-anneal microscopy revealed that essentially no

ruthenium had penetrated the UO_2 single crystal. The experiment demonstrated that the dissolution and diffusion in the polycrystalline ceramic occurred through the grain boundaries.

Analysis of the surface after each polishing step by x-ray fluorescence gave the average ruthenium-to-uranium atom ratio over an area of $\sim 1\ cm^2$. This ratio is equal to the volumetric Ru/U ratio, so that the ruthenium concentration distribution normal to the initial plane of metal was measured. A typical distribution is shown in Fig. 7, in which the solid curve represents the solution to the diffusion equation for an inexhaustible plane source into an infinite medium (12):

$$C(z,t) = C_o \text{erfc}\left[\frac{z - z_o}{2\sqrt{Dt}}\right] \qquad (1)$$

where $C(z,t)$ is the ruthenium/uranium ratio at distance z from the original (visual) interface at time t. The quantities C_o and D are the apparent solubility and effective diffusivity of ruthenium in UO_2, respectively. For each isothermal annealing experiment of the type represented by Fig. 7 the ruthenium distribution was fitted to Eq(1) by choosing values of C_o, D and z_o which provided the best fit to the data points. In all cases the data were nearly perfectly symmetric about the visual interface. Fitting by Eq(1) gives the symmetry position z_o implied by the ruthenium concentration distribution data, which was never different from the visual interface by more than 50 μm.

Table 1 summarizes the results of this data fitting procedure for the seven experiments performed. All but No. 8-15 utilized two or three specimens, each containing ruthenium metal powder, which were annealed simultaneously in the apparatus shown in Fig. 2. Occasionally experimental difficulties resulted in the loss of one specimen in a group (Nos. 11-4 and 11-7). Experiment 7-14 was conducted with molybdenum fittings (alignment tube and separator) in contact with the UO_2 specimens. The remaining experiments employed tungsten hardware throughout. The ends of the pellet stack in Fig. 2 were usually protected by rhenium foils. However, in the last two experiments (11-7 and 11-12), the bottom specimen in the stack was in contact with the molybdenum yoke. In the other experiments, the specimens represent replications. The table also shows the effective diffusivities and apparent solubilities of ruthenium in UO_2 deduced from the concentration distributions of the 13 specimens contained in the seven experiments. The last column of the table gives numbers which are proportional to the sum of the squares of the deviations of the theoretical curve from each data point, and are measures of the goodness of the fits. These numbers show that the fit seen in Fig. 7 is about average for the lot.

The effective diffusivities from Table 1 are plotted in Arrhenius fashion in Fig. 8. There is a clear separation of the values of D deduced from experiments in which the UO_2 contacted only tungsten and those in which the containment metal was totally or partially molybdenum. In the form:

$$D = D_o e^{-E_d/RT} \qquad (2)$$

the pre-exponential factor D_o and the activation energy E_d are 160 cm^2/s and 128 kcal/mole, respectively, for the data with tungsten encapsulation (line b)

and 0.3 cm^2/s and 83 kcal/mole for specimens in contact with molybdenum (line a).

The apparent solubilities plotted in Fig. 9, on the other hand, show no dependence on the container metal and can be represented by:

$$C_o = 7x10^{10} \exp(-147{,}000/RT) \qquad (3)$$

The major features of the results of our experiments which differ from those of the two previous studies of the same phenomenon (9,10) are: 1. The dissolution of micron-size particles of pure ruthenium in UO_2 and transport by grain boundary diffusion in the oxide, and 2. The re-appearance of the ruthenium in the grain boundaries as a metal phase in conjunction with uranium.

Of the many known U-Ru intermetallic compunds, URu_3 is especially stable (13,14) and is probably what we observed in the grain boundaries of the UO_2 specimens after isothermal annealing. This compound (in conjunction with the Rh and Pd analogs) has been found in irradiated oxide fuels as well (4,15). The conditions required for the formation of URu_3 are determined by the thermochemistry of the reaction:

$$UO_{2-x}(s) + 3Ru(s) \rightleftharpoons URu_3(\ell) + \frac{2-x}{2} O_2(g) \qquad (4)$$

which leads to the relation (11):

$$\Delta G^o_{fURu_3} = \Delta G^o_{fUO_2} + \frac{1}{2}\int_0^x \Delta\overline{G}_{O_2}\, dx' - \frac{2-x}{2}\Delta\overline{G}_{O_2} \qquad (5)$$

where $\Delta G^o_{fURu_3}$ and $\Delta G^o_{fUO_2}$ are the standard free energies of formation of URu_3 (13) and UO_2 (16), respectively, and $\overline{\Delta G}_{O_2}$ is the oxygen potential of UO_{2-x}. Since the latter is a known function of stoichiometry x and temperature T (17), Eq.(5) gives the critical O/U ratio (for specified temperature T) at which Ru and URu_3 coexist in UO_{2-x}. If the oxide is more hypostoichiometric than the critical composition, URu_3 is the stable form; for O/U ratios larger than the critical

value, elemental ruthenium is stable. Solution of Eq.(5) gives critical O/U ratios of 1.999 at 2020 K and 1.990 at 2450 K.

The observation of a U-Ru compound in the annealed specimens therefore implies that the urania was substantially hypostoichiometric during the experiments. Although the experiments were conducted in a reducing atmosphere (4% H_2 in Ar), the refractory metal fittings which contained the specimen in the furnace were probably primarily responsible for the reduction of the oxide. The dominance of the refractory metal container over the hydrogen atmosphere in reducing the oxide is supported by the observation of URu_3 in specimens annealed in vacuum. Since the intermetallic compound forms only in hypostoichiometric oxide and the only reductant present in the vacuum experiments was the refractory metal, the latter is implicated as the oxygen sink. Although high-temperature thermodynamic data indicate that stoichiometric UO_2 cannot oxidize Mo to MoO_2 at the temperatures of the experiments in this study, the oxygen potential of the metal which contains less oxygen than the terminal solubility value for the Mo/MoO_2 couple could be lower than that of UO_2. For example, the oxygen potential of a metal with an oxygen concentration 1% of the terminal saturation value would, at 2500 K, be ~46 kcal/mole lower than that of the metal-metal oxide couple, assuming that Sievert's law applied to oxygen solution in the metal. Given the large ratio of refractory metal to urania in the apparatus of Fig. 2, it is very likely that the refractory metal hardware was not saturated with oxygen and was therefore capable of appreciable urania reduction without achieving the terminal solubility. For the range of temperatures shown in Table 1 (2060 to 2300 °C) the terminal solubility varies from 0.2 to 0.7 atom percent (18). The mass of refractory metal in the hot zone of the furnace in the present experiments was ~ 300 g while the mass of two UO_2 pellet wafer specimens was ~ 20 g. If the refractory metal was oxygen-free at the start and the urania initially stoichiometric, saturation

of the metal with oxygen would result in reduction of the O/U ratio of the specimens to 1.90 at 2060 °C and 1.68 at 2300 °C. These large reductions are never achieved because as oxygen is transferred from the UO_2 to the metal, the oxygen potential of the former falls and that of the latter rises. Using available thermodynamic data for UO_{2-x} and for the Mo/MoO_2 couple at 2060 °C, the oxygen potentials of the ceramic and metal phases are equal when the urania has been reduced from an O/U of 2.00 to 1.999 and the initially oxygen-free metal has absorbed $\sim$ ½% of the terminal solubility oxygen content. Post-anneal stoichiometries were determined by measuring the specimen weight gain following several hours of contact with an H_2O/H_2 gas mixture (dew point of 7.5 °C) at 1300 °C (19). The O/U ratios of samples 7-14 (molybdenum encapsulated) and 9-12 (tungsten encapsulated) were 1.996 and 1.998, respectively. These deviations from stoichiometry are not large, probably because the stepwise polishing operation

used to obtain the ruthenium distribution in the specimens employed water as a lubricant and because the specimens had been stored in air for several months between the experiment and the O/U measurement. Nonetheless, the specimens are at least hypostoichiometric and the one which had been contained in molybdenum hardware is more so than the one held in tungsten fittings.

The arguments presented above are consistent with the lack of URu_3 formation in the experiments of D'Annucci et al. (9). Their apparatus consisted of a stack of UO_2 pellets clamped at the ends of tungsten electrodes for direct resistance heating. The sides of the pellet stack did not contact a metal. The environment in this system was much less reducing than ours, so the absence of URu_3 formation in D'Annucci's experiments is understandable.

The basic picture of the ruthenium interaction with urania which emerges from the evidence presented above is as follows.

1. During annealing, the uranium dioxide specimen, which is undoubtedly slightly hyperstoichiometric at the start, is reduced by oxygen absorption by the refractory metal container. During this initial stage of reduction, the oxide is not sufficiently hypostoichiometric to permit URu_3 formation. However, some ruthenium dissolves and diffuses in the grain boundaries of the oxide. Because of the small capacity of the grain boundaries for storing foreign atoms, ruthenium transport during this stage is not detectable experimentally.

2. When the O/U ratio of the specimen reaches the critical value, ruthenium in the grain boundaries starts to react with uranium in the UO_{2-x} to form URu_3.

3. As the reaction proceeds, URu_3 layers build up around the grains of the oxide (Fig. 6). The reaction is supplied with ruthenium by diffusion of this element from the source plane along the interface between the growing URu_3 layers and the shrinking UO_{2-x} grains. The growth of the URu_3 layer is controlled either by the kinetics of the foward reaction of Eq. (4) or by ruthenium diffusion

in the URu_3/UO_{2-x} interface; these are sequential steps in the mechanism. Uranium ion diffusion in the urania lattice is not required because reaction (4) occurs at the URu_3/UO_{2-x} interface. The oxygen liberated by the reaction quickly diffuses into the bulk UO_{2-x} from which it is removed by the refractory metal sink.

4. URu_3 formation continues as long as the original ruthenium layer is not exhausted and as long as the refractory metal sink is capable of maintaining the stoichiometry of the oxide below the critical value. The model implies, and microscopic observation confirms, that the URu_3 layers are thickest near the original plane of ruthenium powder. URu_3 has an fcc crystal structure, and like the pure noble metals, is probably quite impervious to oxygen. Thus, once a sufficiently thick layer of URu_3 surrounds a grain of UO_{2-x}, the reaction ceases because there is no longer any means of removing the reaction product oxygen. The reaction-blocking effect of the URu_3 layer leads to an apparent "solubility" of ruthenium in urania. This "solubility" does not depend on the type of refractory metal which contains the specimens, which determines only how rapidly the URu_3 layers grow. In conformity with the observations, the model predicts that the apparent solubility (C_o) should be the same for both container metals. However, the more effective oxygen removal by molybdenum leads to more widespread URu_3 production in the specimen, which appears as a larger effective diffusion coefficient (D).

Fitting the ruthenium penetration data to simple diffusion theory by the use of Eq. (1) does not mean that the apparent solubility or the effective diffusivity apply to the actual physical processes which the names imply. The pseudoproperties C_o and D contain influences of all of the physical processes involved in the transport of ruthenium in the oxide, including ruthenium grain boundary diffusion, oxygen absorption by the refractory metals, the chemical

kinetics and thermodynamics of reaction (4), and the permeability of URu_3 to oxygen. Fitting the ruthenium penetration data by Eq. (1) is analogous to describing rare gas diffusion in solids with trapping or carbon diffusion in austenite with carbide precipitation by effective diffusion coefficients. Such parameters may be useful correlation constants, but they mask the complexity of the actual processes contributing to the total transport.

V. THERMAL GRADIENT ANNEALING OF UO_2 CONTAINING RUTHENIUM

In order to investigate the transport of ruthenium in UO_2 in a temperature gradient, several ruthenium-loaded UO_2 specimens contained in the crucible of Fig. 4 were tested in a temperature gradient. The experimental procedure was that described in Section II except for omission of the isothermal sintering step. The temperature gradient anneals lasted from 12 to 36 hours. The UO_2 samples were removed from the crucible then polished and analyzed by x-ray fluorescence in the same manner as applied to the specimens from the isothermal anneals. Visual examination of the polished surfaces of the specimens from the thermal gradient experiments revealed ruthenium in the grain boundaries in the form shown in Fig. 6. However, the URu_3 inclusions were concentrated in the central portion of the UO_2 rather than spread uniformly over the entire radius as was found in the isothermal annealing experiments. This phenomenon was probably caused by the presence of a radial as well as an axial temperature gradient. The radial nonuniformity of the Ru/U ratio was averaged out by the large detection area of the x-ray fluorescence spectrometer.

A typical ruthenium distribution from the temperature gradient annealing tests as shown in Fig. 10. The asymmetry of this distribution with respect to the initial source plane could arise from two phenomena. First, the temperature

dependence of the diffusion coefficient favors ruthenium penetration of the hot side of the specimen. Second, the thermal diffusion effect (with a negative Soret coefficient) would augment the asymmetry arising from the temperature dependence of the diffusion coefficient. To determine if the simple effective diffusivity model which successfully correlated the isothermal penetration data could also fit the distributions obtained in a temperature gradient, the following equations was solved numerically:

$$\frac{\partial C}{\partial t} = \frac{\partial}{\partial z}\left\{ D(T)\left[\frac{\partial C}{\partial z} + \frac{CQ^*}{RT^2}\frac{dT}{dz}\right]\right\} \qquad (6)$$

with $C(z, 0) = 0$

$C(z_o, t) = C_o$

$C(\infty, t) = 0$

where D(T) is the effective diffusivity given by Eq. (2) and C_o is the apparent solubility at the temperature of the source plane. Figure 11 shows three solutions of this equation. The solid curve neglects thermal diffusion and assumes that ordinary diffusion is not activated. This is just the symmetric solution given by Eq. (1). The dotted curve neglects thermal diffusion but takes the diffusion coefficient from line b of Fig. 8. The dashed curve adds thermal diffusion with $Q^* = -100$ kcal/mole to the computation. The results shown in Fig. 11 indicate that neither of the effects introduced by the presence of the temperature gradient alter the symmetric concentration distribution significantly. Clearly, modifying the simple effective diffusion model to account for a temperature gradient fails to reproduce even qualitatively the marked asymmetry of the experimental data in Fig. 10, particularly the maximum in the Ru/U ratio at the position nearly 200 μm removed from the source plane.

VI. CONCLUSIONS

Testing of micron-size tungsten and ruthenium particles in UO_2 under isothermal or temperature gradient conditions has revealed the following behavior.

1. Tungsten (or molybdenum) particles of 1 to 10 μm diameter do not migrate in UO_2 when subjected to a temperature gradient of ∿ 1400°C/cm at a temperature of ∿ 2500°C.

2. Ruthenium particles react with hypostoichiometric urania to produce an intermetallic compound which is probably URu_3. The reaction occurs with simultaneous spreading of the ruthenium reactant through the urania. The mechanism is believed to involve diffusion of elemental ruthenium in the grain boundaries of the ceramic with simultaneous reaction to produce free oxygen and the U/Ru intermetallic compound. The URu_3 product grows as a layer in the grain boundaries where the reaction occurs and the oxygen liberated by the reaction diffuses rapidly through the oxide to the refractory metal container. The reaction stops locally when the grains become coated with a layer of URu_3 which prevents removal of the oxygen product. Despite the complexity of the mechanism, the isothermal spreading of ruthenium from an initial source plane can be satisfactorily modeled as a simple diffusion process.

3. The behavior of ruthenium in uranium dioxide subject to a temperature gradient is characterized by significant movement of ruthenium to the hot zones of the ceramic. Transport is also accompanied by formation of the U/Ru intermetallic compound. Ruthenium spreading in urania in a temperature gradient cannot be rationalized by a simple diffusion model, even with a substantial Soret contribution.

ACKNOWLEDGEMENT

The authors are grateful to R. Adamson and Clyde Berry of the Vallecitos Laboratory of the General Electric Company for providing the UO_2 samples for this research. R. Singh of ANL and W.J. McCreary of LASL provided assistance in certain aspects of the experiments and their help is acknowledged. This work was supported by the Director, Office of Energy Research, Office of Basic Energy Sciences, Materials Sciences Division of the U.S. Department of Energy under contract # W-7405-ENG-48.

REFERENCES

1. B.T. Bradbury, J.T. Demant, P.M. Martin and D.M. Poole, J. Nucl. Mater. 17 (1965) 227.
2. B.M. Jeffery, J. Nucl. Mater. 22 (1967) 33.
3. D.R. O'Boyle, F.L. Brown and J.E. Sanecki, J. Nucl. Mater. 29 (1969) 27.
4. J.I. Bramman, R.M. Sharpe, D. Thom and G. Yates, J. Nucl. Mater. 25 (1968) 201.
5. J.H. Davies, R.F. Boyle, B. Weidenbaum and J.E. Hanson, Trans. Amer. Nucl. Soc. 9 (1966) 63.
6. H. Kleykamp, International Conference on Fast Breeder Reactor Fuel Performance, Proc. Symp. (Monterey, Ca. 1979) 393.
7. D.R. O'Boyle, F.L. Brown and A.E. Dwight, J. Nucl. Mater. 35 (1970) 257.
8. F.A. Nichols, J. Nucl. Mater. 84 (1979) 1.
9. F. D'Annucci, C. Sari and G. Schumacher, Nucl. Technol. 35 (1977) 80.
10. L.C. Michels and R.B. Poeppel, J. Appl. Phys. 44 (1973) 1003.
11. R. Yang, "The High Temperature Behavior of Metallic Inclusions in Uranium Dioxide", LBL-11117 (1980).
12. J. Crank, "The Mathematics of Diffusion", 2nd Ed., Oxford (1975).
13. H. Holleck and H. Kleykamp, J. Nucl. Mater. 35 (1970) 158.
14. H. Holleck, J. Nucl. Mater. 42 (1972) 278.
15. F.T. Ewart, J.M. Horspool and G. James, J. Nucl. Mater. 61 (1976) 254.
16. T.L. Markin, Chemical Engineering Progress Symposium Series, Nuclear Engineering, Part XVIII, Vol. 63, No. 80, p. 43, American Institute of Chemical Engineers, New York, (1967).
17. P.E. Blackburn, J. Nucl. Mater. 46 (1973) 244.
18. S.C. Srivastava and L.L. Seigle, Met. Trans., 5, 49 (1974).
19. K.C. Kim, "Oxygen Diffusion in Hypostoichiometric Uranium Dioxide", LBL-11095 (1980).

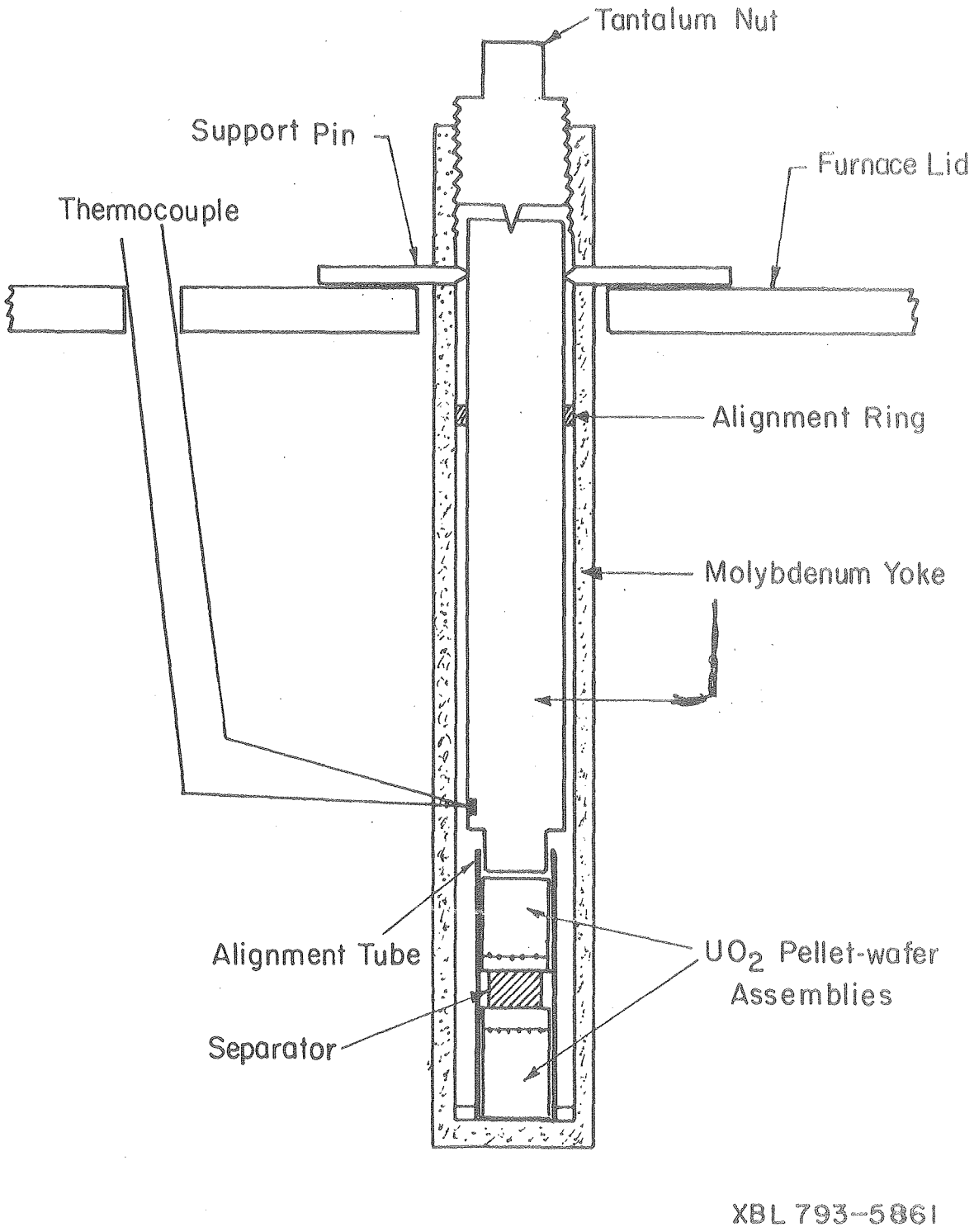

Figure 1 Sintering yoke for UO_2 pellet-wafer assembly.

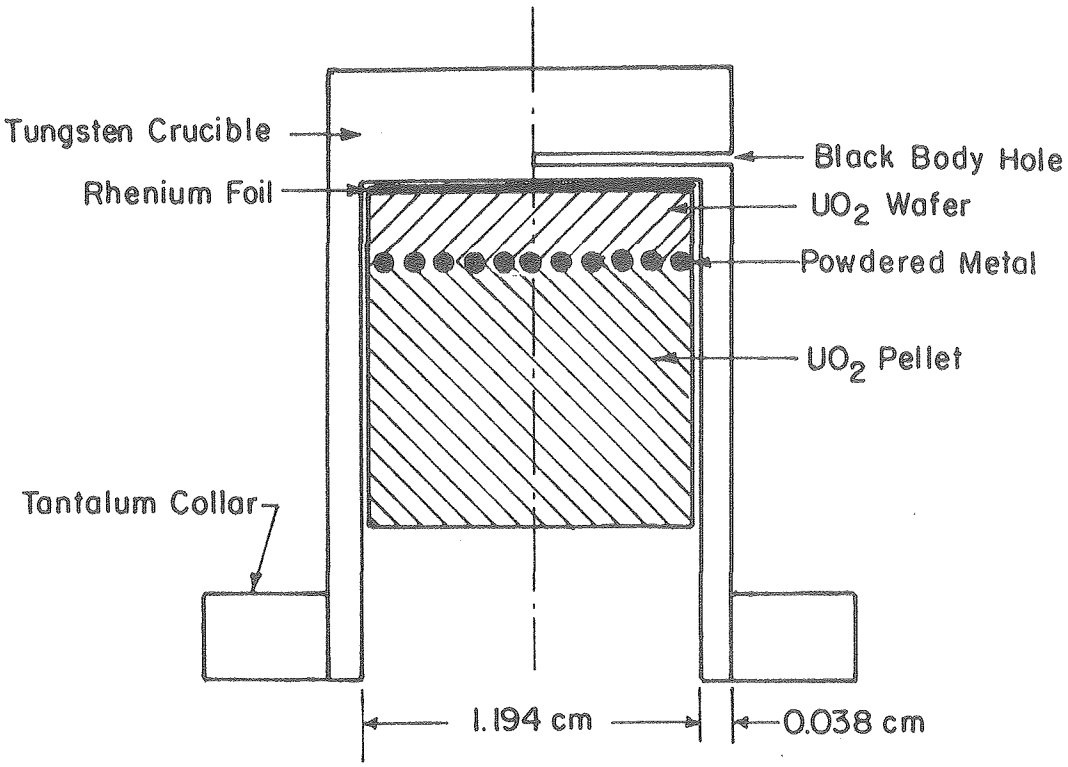

Fig. 2 Tungsten crucible with UO_2 pellet-wafer assembly for use in the temperature gradient furnace.

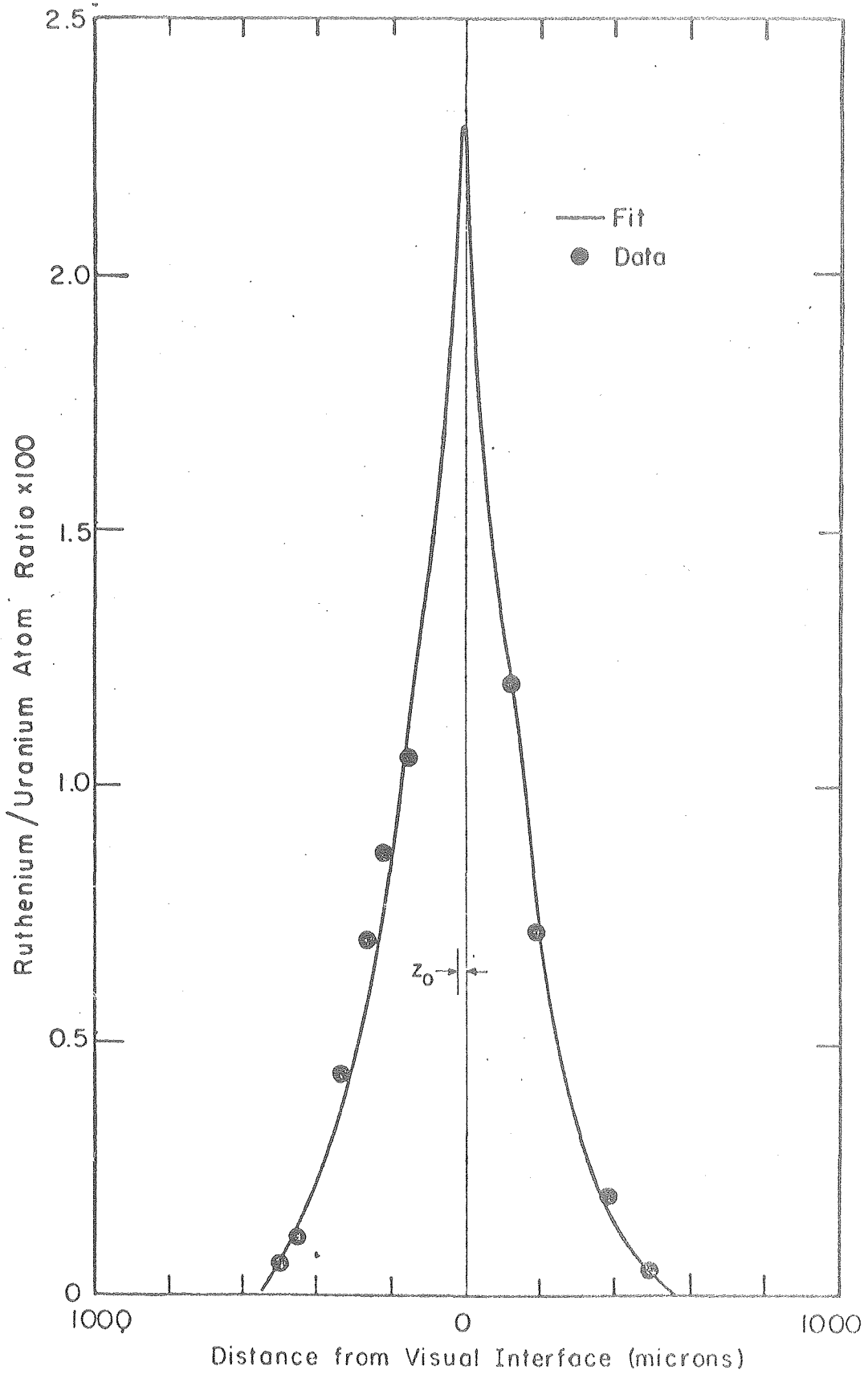

Fig. 3 Ruthenium distribution

XBL 807-5602

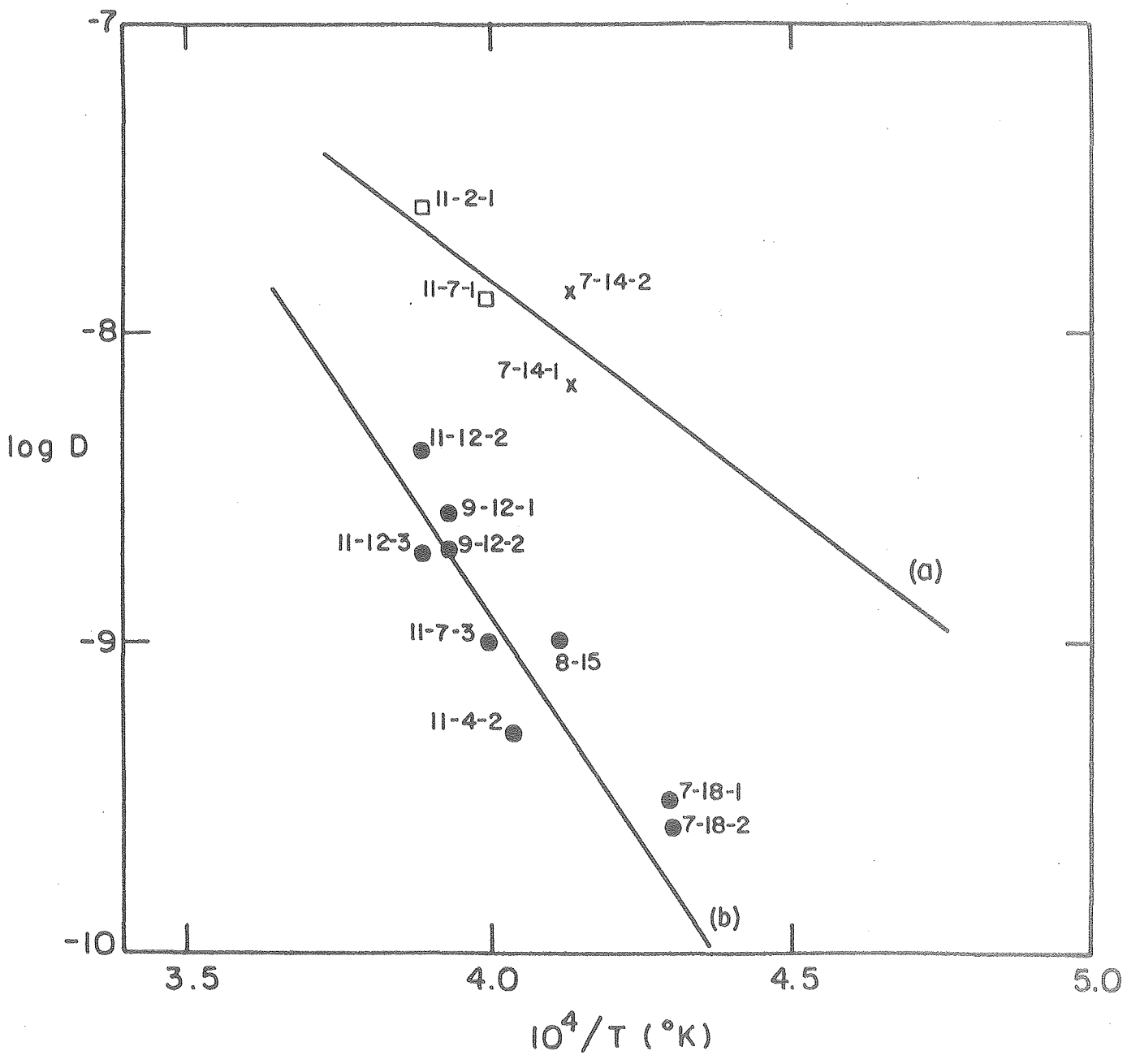

Fig. 4 Effective diffusivity of ruthenium in UO_2

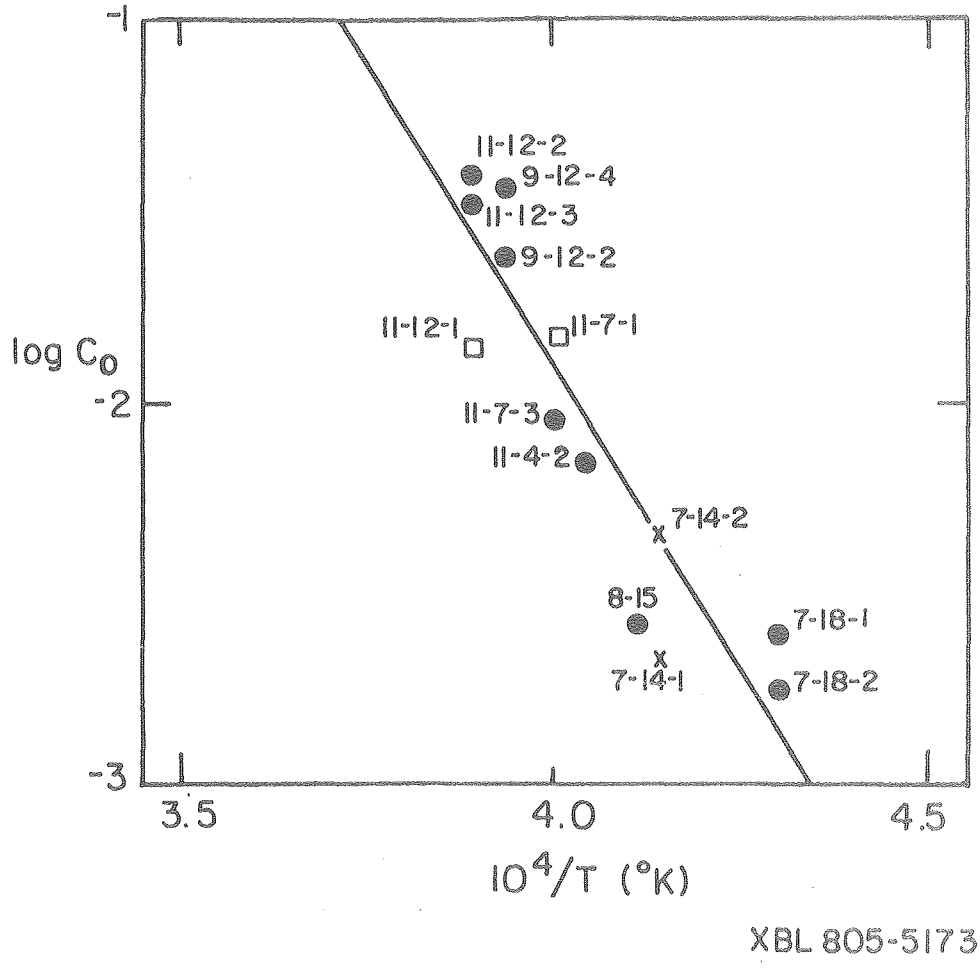

Figure 5 Apparent solubility of ruthenium in UO_2